

## RESEARCH ARTICLE

[View Article Online](#)  
[View Journal](#) | [View Issue](#)

Cite this: *Med. Chem. Commun.*,  
2019, 10, 227

## Prospective treatment of Parkinson's disease by a siRNA–LDH nanoconjugate

Rituparna Acharya,<sup>a</sup> <sup>\*,a</sup> Monisha Chakraborty<sup>a</sup> and Jui Chakraborty<sup>b</sup>

In the world, among the neurodegenerative diseases, Parkinson's is the second most common disease. Although several medications are available in the market, this disease still remains incurable and only the symptoms are controlled to a certain extent with severe side effects. For these reasons we decided to search for a novel therapeutic measure. The objective of this publication was to find a therapeutic procedure to cure this devastating disease. In this study, a biocompatible, easily permeable, cationic nanoparticle-layered double hydroxide was synthesized. Within the layers of these nanoparticles we intercalated  $\alpha$  synuclein siRNA, which helps to silence the  $\alpha$  synuclein gene. After the intercalation, which was optimized at a 1:40 ratio of siRNA:(LDH), we studied its stability in blood by a RNase protection test and serum protection assay. Both proved that LDH was an excellent nanocarrier that can protect intercalated molecules within its layers. After that, several cellular studies were performed by FACS to evaluate its biocompatibility after intercalation and cellular internalization. Results of the biocompatibility studies found it to be nontoxic and in the cellular internalization study, 51.55% of cells were taken into the nanoconjugate and confocal microscopy supported the data from FACS. Lastly, ELISA was performed to discover protein levels in the control, overexpressed, and treated groups of the SH-SY5Y cell line. These results verified that this nanoconjugate is a protective treatment procedure for Parkinson's disease.

Received 4th October 2018,  
Accepted 8th December 2018

DOI: 10.1039/c8md00501j

[rsc.li/medchemcomm](http://rsc.li/medchemcomm)

## 1. Introduction

In this world, Parkinson's disease is the second most common neurodegenerative disorder and 15 to 328 persons among 100 000 are found to be affected by it. The most common symptoms are resting tremor, bradykinesia, posture instability, and rigidity. Cigarette smoking, alcohol consumption, and some types of pesticides and herbicides are the prevalent factors that lead to this disease condition. However, genetic risk factors cannot be ignored.<sup>1</sup>

Alpha-synuclein ( $\alpha$ -syn) is a protein which remains in the presynaptic neurons that are linked with Parkinson's disease as a genetic and neuropathological cause of the disease and this protein also has been found to be responsible for neurological deaths by forming protofibrils. Moreover, the secretory  $\alpha$ -syn can cause deleterious effects in associated cells and contribute to disease progression.<sup>2</sup>

Currently, there are 5 groups of drugs which are prescribed for treatment of Parkinson's disease. These are: (i) levodopa plus a peripheral decarboxylase inhibitor, (ii) aman-

tadine, (iii) anticholinergic drugs, (iv) selegiline, and (v) dopamine agonists. Among these, levodopa is considered to be the most effective. In combination with selegiline, however, it helps retard disease progression, although it can produce serious motor complications.<sup>3</sup> But, whichever drugs are used, the disease cannot be cured totally and is only retarded in its progress, in addition to severe side effects.

RNAi therapy is a currently upcoming way of combating these types of genetic diseases.<sup>4–6</sup> Overexpression of the  $\alpha$  syn gene was found to be involved in the pathogenesis of Parkinson's disease but the restoration of normal protein level, which is the byproduct of this gene, can be maintained by a RNAi therapeutic mechanism. Small interfering RNAs (siRNAs) are those types of ribonucleic acids which help in gene silencing and are capable of controlling overexpressed  $\alpha$ -syn gene to a normal level.<sup>7,8</sup> However, in spite of the beneficial effects of this siRNA, it cannot be used in its bare form because the transfection efficiency of these macromolecules is poor. Moreover, they are not permeable to the blood/brain barrier and are degradable in blood in their bare form.<sup>9</sup> Because of these shortcomings, an efficient, biocompatible delivery vehicle is of utmost necessity to combat this disease.<sup>10</sup>

These aforesaid criteria are fulfilled by a most promising biocompatible, low cost, easy to make nanodelivery vehicle as a layered double hydroxide (LDH).<sup>11</sup> Moreover, this nanoparticle has a hexagonal structure with cationic layers. The

<sup>a</sup> School of Bioscience and Engineering, Jadavpur University, 188, Raja S.C. Mullick Road, Kolkata 700 032, India. E-mail: [rituparnaacharya@rediffmail.com](mailto:rituparnaacharya@rediffmail.com); Tel: +91 8017071353

<sup>b</sup> CSIR-Central Glass and Ceramic Research Institute, 196 Raja S. C. Mullick Road, Jadavpur, Kolkata-700 032, India

anions between these layers can be readily exchanged with any other anion-like drugs or DNA or RNA (siRNA, shRNA, miRNA) biomolecules.<sup>12–14</sup> As these biomolecules are anionic in nature, they are quite stable within these layers and highly stable in blood/serum or can escape any degradable enzymatic action.<sup>15–17</sup> Hence, the objective of our study was to design a non-viral nanovehicle, Mg–Al-LDH,<sup>18–22</sup> for delivery of  $\alpha$ -syn siRNA, which can be a potential curative therapeutic approach for Parkinson's disease.

## 2. Methodology

### 2.1. Synthesis of layered double hydroxide nanoparticles

A 500 mL solution was prepared containing  $\text{Mg}(\text{NO}_3)_2 \cdot 6\text{H}_2\text{O}$  (32 mmol) and  $\text{Al}(\text{NO}_3)_3 \cdot 9\text{H}_2\text{O}$  (16 mmol) under vigorous stirring using a magnetic stirrer at 1100 rpm under a stream of nitrogen. Then, 100 mL of NaOH (0.5 N) was added drop wise to this mixed metal solution until the final pH reached 11.5. The resultant solution was aged at 25 °C for 24 h, and then centrifuged at 8519g rcf for 15 min (Heal Force, Neofuge 15R, China). The precipitate obtained was separated and washed several times with decarbonated water. Then, the resultant precipitate was freeze dried (EYEL4, FDU2200, Japan) at –82 °C and 20 Pa pressure, resulting in a fine, free flowing nanocrystalline LDH powder with a size range of 100–200 nm.

The LDH nanoparticles obtained were characterized using X-ray diffraction, particle size analysis, FESEM, *etc.*

### 2.2. siRNA intercalation in LDH

The  $\alpha$ -syn siRNA sense strand sequence corresponds to 5'-CCAAAGAGCAAGUGACAAA-3' (M/S Dharmacon, USA). The siRNA and Mg–Al-LDH nanoparticles were mixed in various mass ratios ranging from 1 : 10 to 1 : 60<sup>23</sup> and deionized water was added to make a final volume of 10  $\mu\text{L}$ , keeping the final siRNA concentration constant at 0.1  $\mu\text{g } \mu\text{L}^{-1}$ . Samples were incubated at 37 °C for 30 min after which an appropriate amount of RNA loading buffer was added to each sample. Gel electrophoresis was carried out on 3.0% agarose gels (TBE buffer, 1% ethidium bromide) at 80 V for 45 min and the gels were subsequently imaged using a gel documentation system (M/S BioradEZ imager, USA).

### 2.3. Stability studies

**2.3.1. RNase protection assay.** After determining the best  $\alpha$ -syn siRNA–LDH ratio to form intercalates, 1  $\mu\text{g}$  of siRNA entrapped in the LDH was incubated with 0.05  $\mu\text{g}$  of bovine pancreatic RNase A (Ambion, Austin, TX, USA) in 50  $\mu\text{L}$  of HEPES (20 mM at pH 7.0) at 37 °C for 1 h. After incubation, a 10  $\mu\text{L}$  aliquot of the previous mixture was added to 30  $\mu\text{L}$  of FA dye (TBE, deionized formamide, triton X-100, PBS, bromophenol blue, and xylene cyanol) to stop the RNaseA reaction. Gel electrophoresis was performed using 3% agarose gel. For comparison and testing effects of enzyme on the naked siRNA, the same enzyme was incubated with bare siRNA for

the same periods, followed by enzyme inactivation and gel electrophoresis.

**2.3.2. Serum protection assay.** Equal amounts of the intercalates and RPMI medium containing 10% FBS were incubated together at 37 °C for 24 and 48 hours. The serum effect was terminated by incubating the mixtures in a water bath at 60 °C for 10 min, followed by centrifugation for 10 min at 10 000 RPM and testing the stability using gel electrophoresis.

### 2.4. Cell culture

A SH-SY5Y cell line (neuroblastoma) procured from NCCS, Pune was cultured in the laboratory. RPMI-1640 media (AL-162S, HIMEDIA) supplemented with 10% FBS and 1% antibiotic was used to culture the cells which were kept at 37 °C with 5%  $\text{CO}_2$ .

### 2.5. Cytotoxicity and cell proliferation assay

Proliferation of cells was assessed using an *in vitro* toxicological assay kit XTT (Sigma Aldrich, USA) according to the manufacturer's protocol. Briefly, cells were seeded in a 6-well plate at  $1 \times 10^6$  cells per well with treatment by 1, 5, 10, 15 and 20  $\mu\text{g}$  of intercalated siRNA per 2.5 mL media with a ratio of 1 : 40 RNA : LDH for 24 h. Reconstituted XTT solution was added at 20% of the culture volume and incubated for 4 h at 37 °C with 5%  $\text{CO}_2$ . Then, it was transferred into a 96-well plate and absorbance was measured at 450 nm.

### 2.6. FACS analysis

For flowcytometry measurements, cells were seeded in a 6-well plate at  $1 \times 10^6$  cells per well and treated with 10 and 20  $\mu\text{g}$  of intercalated FITC tagged siRNAs per 2.5 mL media. The cells were incubated for 24 h. After 24 h, cells were centrifuged, and the pellet was washed three times with PBS and subjected to flowcytometry in FACS VERSE (BD Biosciences, USA). For the time dependent study, the cells were plated as before and treated with 10  $\mu\text{g}$  of intercalated FITC tagged siRNAs per 2.5 mL of media for 6, 12, and 18 h. After incubation, the cells were centrifuged and washed with PBS as before and subjected to flowcytometry analysis in FACS VERSE.

### 2.7. Confocal microscopy

For confocal microscopy,  $\alpha$ -syn siRNA–LDH of various concentrations were treated with the untreated control, SH-SY5Y cells were seeded at a density of  $2 \times 10^4$  cells per well in a 96-well plate and incubated for 24 h. After incubation, they were fixed with 4% paraformaldehyde, mounted with DAPI containing mounting media, and images were taken using BD Attovision software.

### 2.8. ELISA

**2.8.1. Cell culture and treatment.** Over expressed  $\alpha$ -syn cell culture and treatment with  $\alpha$ -syn siRNA–LDH nanoconjugate

SH-SY5Y cell and a clone expressing human alpha-synuclein with a C-terminal HA tag (alpha-synuclein-HA) were grown under standard conditions and maintained with G418 ( $0.4 \text{ mg mL}^{-1}$ ).<sup>24</sup> Then, the  $\alpha$ -syn siRNA-LDH conjugate was used for treating the cell line at the previous optimized concentration for 24 h.

**2.8.2. ELISA for  $\alpha$ -syn release quantification.** To quantify  $\alpha$ -synuclein released by the cells at 24 h, the conditioned medium was concentrated with an Amicon Ultra-15 Centrifugal Filter Unit (Millipore, USA). After that, the concentrated medium was sonicated for 20 minutes and  $\alpha$ -synuclein was quantified using an alpha-synuclein ELISA kit (KHB0061, ThermoFisher Scientific, USA) as per manufacturer's protocol.<sup>25</sup>

**2.8.3. ELISA for cellular  $\alpha$ -syn quantification.** Cellular  $\alpha$ -syn was quantified by extracting  $\alpha$ -syn in SDS/urea ( $8 \text{ mol L}^{-1}$  of urea, 2% SDS) and high salt (HS, 50 mmol Tris, 750 mmol NaCl, 5 mmol EDTA), HS/Triton (1% Triton) followed by centrifugation at 16 000g as previously described.<sup>26</sup>

## 3. Results

### 3.1. Characterization of LDH

The PXRD pattern of Mg-Al-LDH nanoparticles (Fig. 1) exhibits a well crystallized hydrotalcite-like phase comprising characteristic (00 $l$ ) reflections indexed to a hexagonal lattice with rhombohedral space group for layered clays. Apart from the diffraction from the (003) plane corresponding to the Mg-Al-LDH system, higher order reflections of (006) and (009) are also visible, confirming a hexagonal system with rhombocentred lattice, matching with the standard JCPDS pattern (JCPDS File No. 35-0964).

The hydrodynamic sizes of Mg-Al-LDH in aqueous solution were measured by light scattering (Fig. 2). The average size of LDH particles in aqueous suspension was 37.84 nm with a polydispersity index (PDI 0.541). It is known that if the size of particles responsible for photon scattering increases by one order of magnitude, then scattered light intensity increases by about a million times. The algorithm in the size measurement software converts the intensity of photon signal to size.

The FESEM image shows well dispersed Mg-Al-LDH nanoparticles, exhibiting globular morphology with a size distribu-

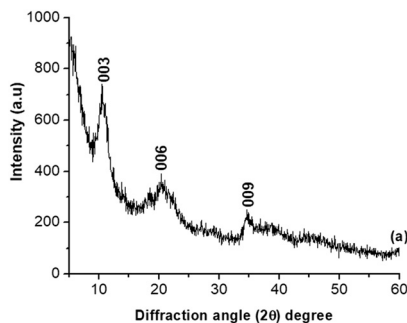


Fig. 1 XRD data of LDH.

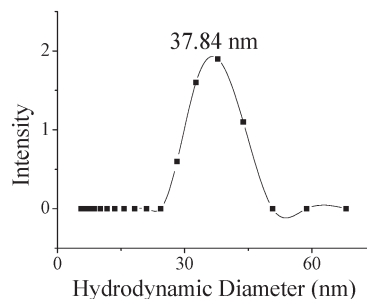


Fig. 2 Particle size of LDH.

tion in the range (30–70 nm) in general, although, in several locations, there are agglomerated clusters, marked by an arrow (Fig. 3).

### 3.2. Intercalation of siRNA and LDH

The siRNA having a complimentary sequence of the  $\alpha$ -syn gene mRNA was used in this study. We specifically used siRNA from M/S Dharmacon for our work. For intercalation, different mass ratios were used from 1:10 to 1:60 RNA:LDH and incubated at 37 °C for 30 minutes followed by subjection to agarose gel electrophoresis.<sup>8</sup> When the siRNA is tightly intercalated within the LDH it becomes unable to move towards the positively charged electrode because the negative charge of the siRNAs becomes obscured by LDH intercalation. This predictive behavior was tested and results are shown in Fig. 4. The intercalation was greater when the presence of LDH was more, and the total siRNA was intercalated in a 1:40 mass ratio. A 40 fold increased amount of LDH was sufficient to retain the siRNA in the gel electrophoresis well (Fig. 4).

### 3.3. Stability studies

The gel electrophoresis technique is still the simplest and most sensitive approach for evaluating stability of a loaded siRNA within its formulation. However, testing the integrity of siRNA requires a method to recover it from the carrier and this differs according to the type and structure of the carrier

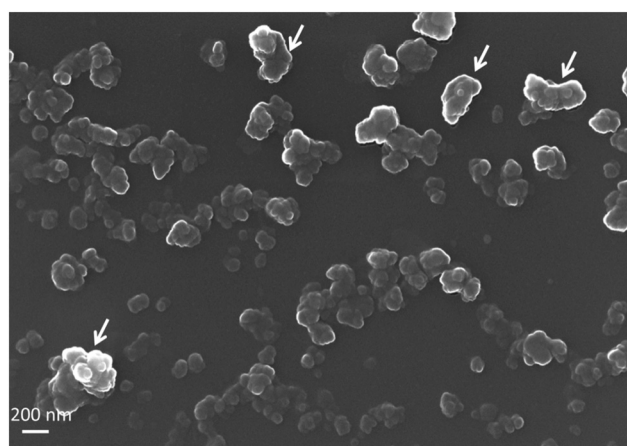


Fig. 3 FESEM image of LDH.

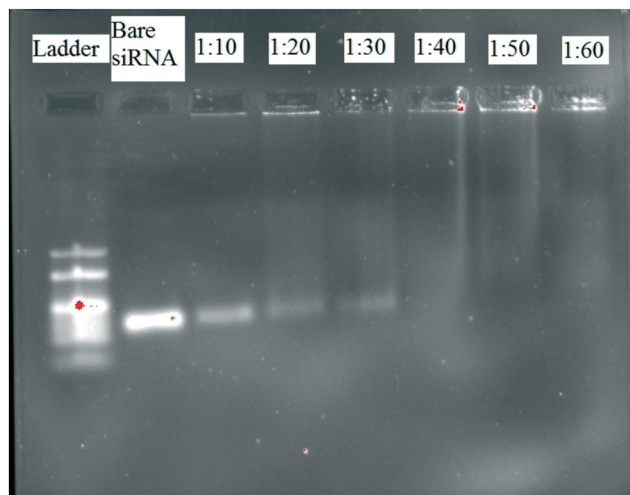


Fig. 4 Assessment of siRNA intercalation by LDH nanoparticles.

as well as molecular weight of the nucleic acid, and sometimes it may lead to degradation of the siRNA itself. In this study, different centrifugation speeds and time periods were employed for recovering loaded siRNA from the LDH nanoparticles. The optimum recovery occurred after centrifugation for 10 min with a speed 10 000 RPM at 37 °C, followed by testing the effect of RNase enzyme and serum components.<sup>27</sup>

The LDH layers should protect the siRNA from degradation by externally added RNase A. Bovine pancreatic RNase A was incubated with siRNA-LDH nanoconjugate to determine its protection by LDH layers. As shown in Fig. 5, gel electrophoresis indicates that free siRNA is degraded (Fig. 5A, lane 4), while siRNA encapsulated in the LDH nanoparticles is completely protected (Fig. 5A, lane 3).

Although the bare siRNA degraded completely after 24 h of incubation in serum catalyzed by its nucleases (Fig. 5B, lane 4), LDH showed good efficiency to protect the

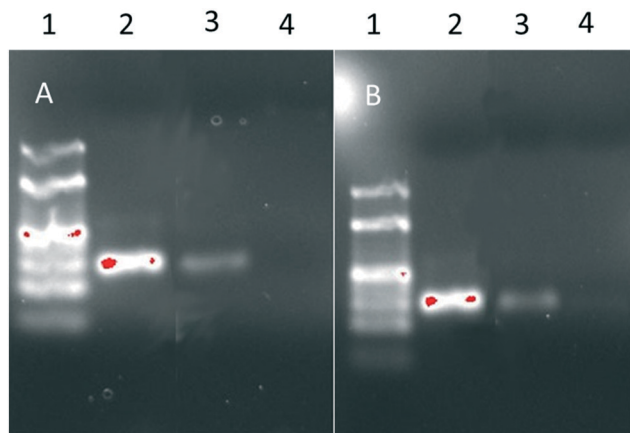


Fig. 5 A) Enzymatic stability study, lane 1: ladder, lane 2: bare siRNA, lane 3: siRNA-LDH nanoconjugate after treatment, and lane 4: bare siRNA after RNase treatment. B) Serum stability study, lane 1: ladder, lane 2: bare siRNA, lane 3: siRNA-LDH nanoconjugate after treatment, and lane 4: bare siRNA after treatment.

siRNA after incubation for 24 h (Fig. 5B, lane 3). This confirms stability of the nanoconjugates in serum and that they can be used in the transfection of mammalian cells in a serum-containing medium.

### 3.4. Cell viability of siRNA-LDH conjugate

Before performing the FACS experiment, we tested the cell viability and proliferation assay for identifying the optimum concentration for treatment with a cellular internalization test. We performed a test of the siRNA-LDH conjugate on the SH-SY5Y cell line, which is the neuroblastoma cell line in our brains. We considered the SH-SY5Y clone E6-1 cell line as the most appropriate for our work. A 6-well plate was seeded with cells and varying concentrations of siRNA-LDH conjugate were added up to 20  $\mu\text{g}$  siRNA: 800  $\mu\text{g}$  LDH per 2.5 mL of media. From a previous publication we had learned that 50  $\mu\text{g mL}^{-1}$  concentration of LDH is the optimum concentration for treatment.<sup>8</sup> Our cell viability experiment demonstrated that there was no significant cell death at concentrations from 40  $\mu\text{g mL}^{-1}$  of LDH to 20  $\mu\text{g mL}^{-1}$  of siRNA conjugated with 800  $\mu\text{g mL}^{-1}$  LDH.

Therefore, we consider that 800  $\mu\text{g mL}^{-1}$  of LDH, in conjugation with a subsequent amount of siRNA, is the maximum amount which should be used for experiments of cellular internalization studies that are both concentration- and time-based (Fig. 6).

### 3.5. Cellular internalization depending upon concentration

The siRNA sequence of the  $\alpha$ -syn gene which we used does not correspond with any other human gene sequence. So, we investigated cellular uptake of the FITC-tagged siRNA-LDH conjugate in the SH-SY5Y cell line. For this purpose, SH-SY5Y cells were seeded in a 6-well plate at a concentration of  $3 \times 10^6$  cells and treated with siRNA-LDH nanoconjugate having the previously mentioned concentration. FACS analysis was performed after 24 h incubation.

The FITC-siRNA-LDH conjugate as demonstrated in Fig. 7 was efficiently internalized by the SH-SY5Y cells and 22.29% of them were found to be FITC positive after 24 h treatment with the siRNA-LDH conjugate (Fig. 7).

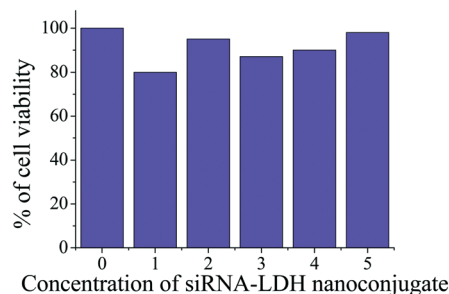


Fig. 6 Cell viability after treating with  $\alpha$ -syn siRNA-LDH nanoconjugate: 0) control, 1) 1  $\mu\text{g}$  siRNA-40  $\mu\text{g}$  LDH, 2) 5  $\mu\text{g}$  siRNA-200  $\mu\text{g}$  LDH, 3) 10  $\mu\text{g}$  siRNA-400  $\mu\text{g}$  LDH, 4) 15  $\mu\text{g}$  siRNA-600  $\mu\text{g}$  LDH, and 5) 20  $\mu\text{g}$  siRNA-800  $\mu\text{g}$  LDH.



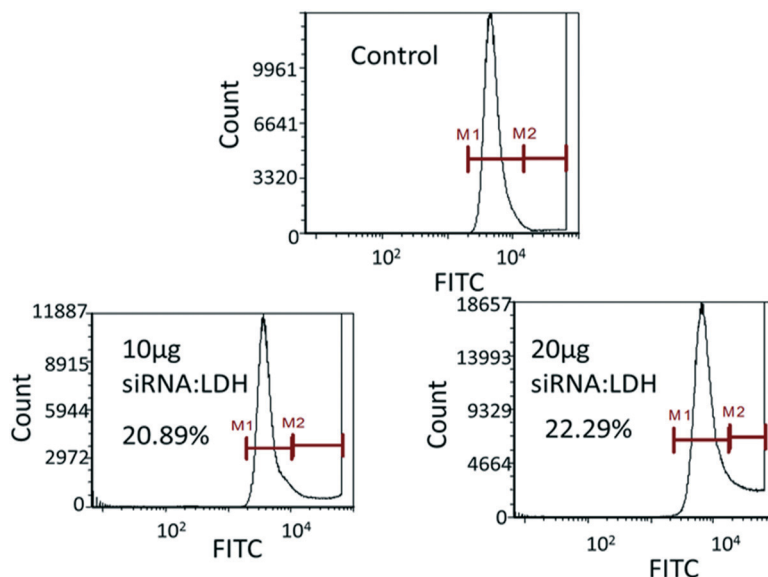


Fig. 7 Flowcytometry of cellular internalization of the FITC-siRNA-LDH conjugate at different concentrations using the SH-SY5Y cell line.

### 3.6. Cellular internalization dependence with time

To find the approximate time required to internalize the  $\alpha$ -syn siRNA-LDH conjugate, SH-SY5Y cells were seeded as before in 6-well plates and treated with various concentrations of the conjugate at different time points, e.g., 6, 12, and 18 h. However, at 6 h the FITC-siRNA-LDH conjugates showed 51.55% uptake which was maximum in the 24 h study. Thus, it can be said that after 6 h the cells released their fluorescence and demonstrated a lesser extent of fluorescent intensity<sup>17</sup> (Fig. 8).

### 3.7. Confocal microscopy

The above observations of cellular uptake of the FITC-tagged siRNA-LDH nanoconjugate, using SH-SY5Y cells, were further

confirmed by confocal laser scanning microscopy (CLSM) images, shown in Fig. 9, which correspond to 24 h post treatment. The accumulation of FITC-containing siRNA-LDH nanoconjugate in the intracellular matrix (both in the phase contrast image and the FITC image), demonstrated their potential applications as a biomarker and corroborated our FACS results corresponding to both time and concentration, indicating potential of the LDH-based carrier to successfully deliver the subject biomolecule to a specific site.

### 3.8. ELISA for quantification of extracellular and intracellular $\alpha$ -syn

Exosomes were isolated from  $\alpha$ -syn overexpressing SH-SY5Y cells from the conditioned medium using an established

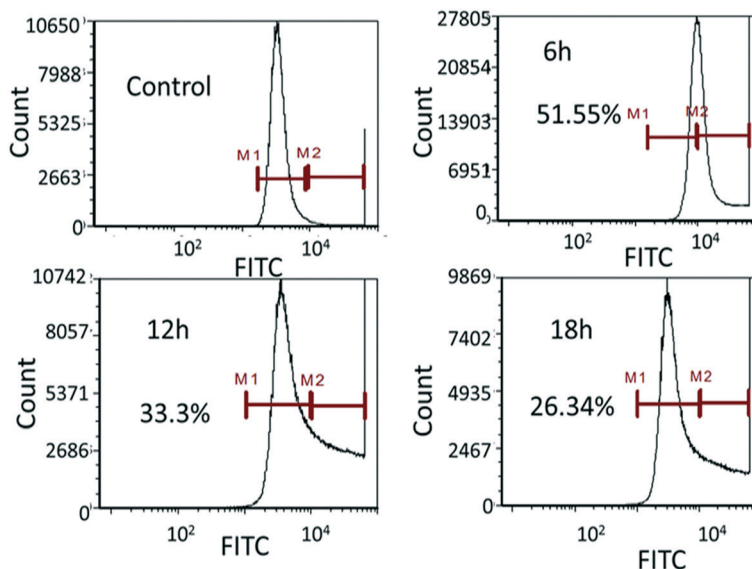


Fig. 8 Flowcytometry of cellular internalization of the FITC-siRNA-LDH conjugate at different times.

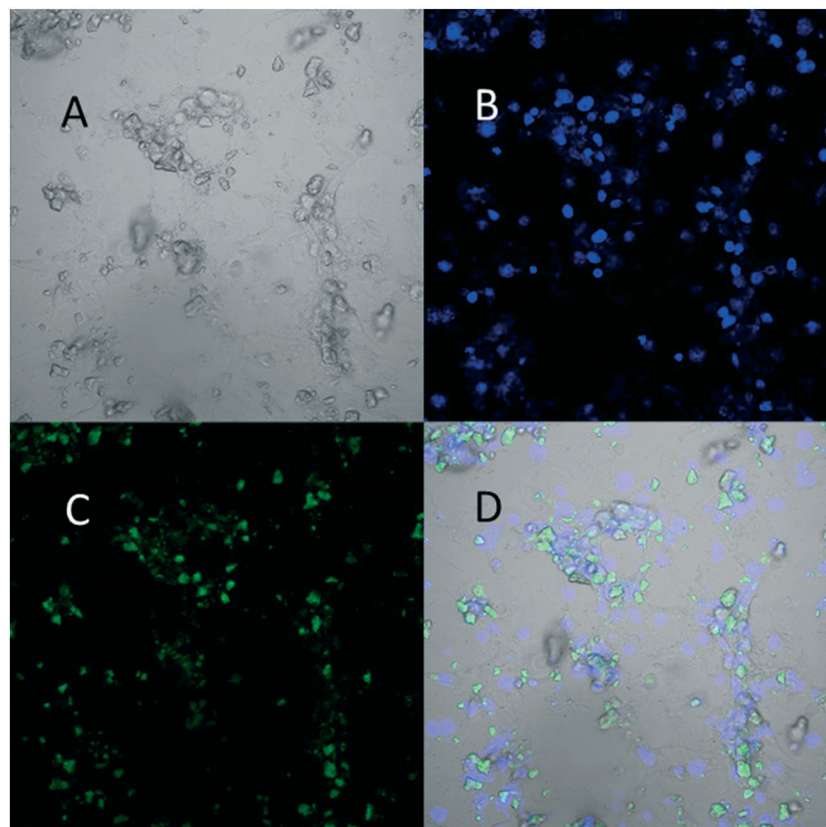


Fig. 9 Confocal microscopy. A) Phase contrast image, B) Dapi image, C) FITC image, and D) fused image.

ultracentrifugation method.<sup>28</sup> However, ELISA analysis demonstrated the  $\alpha$ -syn protein was detectable only in the overexpressed  $\alpha$  syn-HA. After treatment with our  $\alpha$ -syn siRNA-LDH nanoconjugate, the expression level reduced from 100% to 30% (Fig. 10A).

Moreover, the cellular concentration was also checked by ELISA analysis and it demonstrated a significant amount of reduction in the expression of the  $\alpha$ -syn protein level (Fig. 10B).

## 4. Discussion

Although several investigations have been made using different types of siRNAs delivery systems, a suitable delivery sys-

tem is still under research. Chitosan, PEG, PEI, *etc.* nanoparticles have been tried as deliver vehicles for siRNAs but, at present, they still have not been found to be convenient for use *in vivo*.

Thus, potential siRNA technologies for Parkinson's disease treatments still need to be explored. Here, we explored the first study of the  $\alpha$ -synuclein siRNA-LDH conjugate in therapeutic applications for Parkinson's disease. In our study, we demonstrated the stability of the conjugate in presence of RNase enzyme and serum. No toxicity of siRNA-LDH conjugate on the SH-SY5Y cell line resulted and we also showed the cellular internalization of this conjugate. Finally, we have direct evidence that after 6 h of treatment, the conjugate was internalized by the neuroblastoma cells.

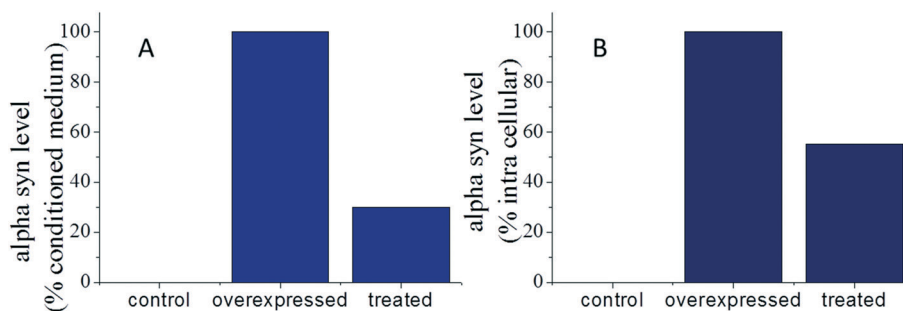


Fig. 10 A)  $\alpha$  syn level in the conditioned medium and B)  $\alpha$  syn level within the cell.

After 6 h of study, the SH-SY5Y cells demonstrated 51.55% internalization of the FITC-siRNA-LDH conjugate, which then gradually decreased with time. Bare siRNA, however, can't enter into a cell as it is negatively charged, and the cell membrane is also negatively charged so they repel each other. But, when this negatively charged siRNA is intercalated within the layered double hydroxide, then its negative charge becomes obscured and the positive charge of the LDH is present on its surface; so, the positive charge on the surface of LDH attracts the negative charge of the cell and, as a result, they are internalized by the cell. This corroborates the principle of the conjugate's uptake by the cell.

## 5. Conclusions

In this study, layered double hydroxide was used as a siRNA delivery vehicle and it demonstrated efficient delivery of siRNA into neuroblastoma cells. In the deadly Parkinson's disease, proper treatment regimens are unavailable, so further study is required to identify an optimum therapeutic strategy for it. A therapeutic measure using  $\alpha$ -synuclein siRNAs will lead to the complete curing of this disease if this conjugate can be delivered frequently to a patient's body. Although further optimization of this therapeutic strategy is required, our study strongly suggests that LDH is an efficient delivery vehicle for  $\alpha$ -synuclein siRNAs in neuroblastoma cells.

## Conflicts of interest

The authors report no declarations of conflicts of interest.

## Acknowledgements

The authors are grateful to the Director, the Central Glass and Ceramic Research Institute, Kolkata, India for providing his permission to carry out the above work. Thanks are due to all other support staff of CGCRI, Kolkata who made this work possible. We also deeply acknowledge the kind help of Dr Sugata Hazra, School of Oceanographic Study, Jadavpur University for his hearty support for the completion of this work.

## References

- 1 S.-Y. Chen and S.-T. Tsai, *Tzu Chi Med. J.*, 2010, **22**, 73–81.
- 2 L. Stefanis, *Cold Spring Harbor Perspect. Med.*, 2012, **2**, a009399.
- 3 R. J. Coleman, *Drugs Aging*, 1992, **2**, 112–124.
- 4 X. Xu, J. Wu, Y. Liu, P. E. Saw, W. Tao, M. Yu, H. Zope, M. Si, A. Victorious, J. Rasmussen, D. Ayyash, O. C. Farokhzad and J. Shi, *ACS Nano*, 2017, **11**, 2618–2627.
- 5 J. Zhou and J. J. Rossi, *Gene Ther.*, 2011, **18**, 1134–1138.
- 6 A. Vermeulen, L. Behlen, A. Reynolds, A. Wolfson, W. S. Marshall, J. Karpilow and A. Khvorova, *RNA*, 2005, **11**, 674–682.
- 7 M. Takahashi, M. Suzuki, M. Fukuoka, N. Fujikake, S. Watanabe, M. Murata, K. Wada, Y. Nagai and H. Hohjoh, *Mol. Ther.–Nucleic Acids*, 2015, **4**, e241.
- 8 K. Ladewig, M. Niebert, Z. P. Xu, P. P. Gray and G. Q. Lu, *Biomaterials*, 2010, **31**, 1821–1829.
- 9 Y. Gelfand and M. G. Kaplitt, *World Neurosurg.*, 2013, **80**, S32.e11–S32.e18.
- 10 A. Z. Wang, R. Langer and O. C. Farokhzad, *Annu. Rev. Med.*, 2012, **63**, 185–198.
- 11 S.-J. Choi, J.-M. Oh and J.-H. Choy, *J. Phys. Chem. Solids*, 2008, **69**, 1528–1532.
- 12 K. Ladewig, Z. P. Xu and G. Q. Lu, *Expert Opin. Drug Delivery*, 2009, **6**, 907–922.
- 13 S. Miyata, *AnionExchange Properties of Hydrotalcite-Like Compounds*, 1983.
- 14 S. J. Choi and J. H. Choy, *Nanomedicine*, 2011, **6**, 803–814.
- 15 C.-H. Chan, J.-K. Chen and F.-C. Chang, *Sens. Actuators, B*, 2008, **133**, 327–332.
- 16 M. J. Masarudin, K. Yusoff, R. A. Rahim and M. Z. Hussein, *Nanotechnology*, 2009, **20**, 045602.
- 17 B. Kim, G. Han, B. J. Toley, C. K. Kim, V. M. Rotello and N. S. Forbes, *Nat. Nanotechnol.*, 2010, **5**, 465–472.
- 18 J. Chakraborty, S. Roychowdhury, S. Sengupta and S. Ghosh, *Mater. Sci. Eng., C*, 2013, **33**, 2168–2174.
- 19 S.-J. Choi, J.-M. Oh and J.-H. Choy, *J. Ceram. Soc. Jpn.*, 2009, **117**, 543–549.
- 20 J. H. Choy, S. Y. Kwak, Y. J. Jeong and J. S. Park, *Angew. Chem., Int. Ed.*, 2000, **39**, 4041–4045.
- 21 S. Ray, A. Mishra, T. K. Mandal, B. Sa and J. Chakraborty, *RSC Adv.*, 2015, **5**, 102574–102592.
- 22 Z. P. Xu, M. Niebert, K. Porazik, T. L. Walker, H. M. Cooper, A. P. Middelberg, P. P. Gray, P. F. Bartlett and G. Q. Lu, *J. Controlled Release*, 2008, **130**, 86–94.
- 23 Y. Wong, K. Markham, Z. P. Xu, M. Chen, G. Q. M. Lu, P. F. Bartlett and H. M. Cooper, *Biomaterials*, 2010, **31**, 8770–8779.
- 24 K. Y. Chau, H. L. Ching, A. H. Schapira and J. M. Cooper, *J. Neurochem.*, 2009, **110**, 1005–1013.
- 25 L. Alvarez-Erviti, Y. Seow, A. H. Schapira, C. Gardiner, I. L. Sargent, M. J. A. Wood and J. M. Cooper, *Neurobiol. Dis.*, 2011, **42**, 360–367.
- 26 E. A. Waxman and B. I. Giasson, *J. Neuropathol. Exp. Neurol.*, 2008, **67**, 402–416.
- 27 B. Balcomb, M. Singh and S. Singh, *ChemistryOpen*, 2015, **4**, 137–145.
- 28 B. J. Quah and H. C. O'Neill, *Blood Cells, Mol., Dis.*, 2005, **35**, 94–110.